Monthly Notices
of the
ROYAL ASTRONOMICAL SOCIETY

MNRAS **460,** 1188–1200 (2016)
Advance Access publication 2016 May 1

doi:10.1093/mnras/stw1029

Bondi accretion in early-type galaxies

Valeriya Korol,[1,2] Luca Ciotti[1]★ and Silvia Pellegrini[1]

[1]*Department of Physics and Astronomy, University of Bologna, viale Berti Pichat 6/2, I-40127 Bologna, Italy*
[2]*Leiden Observatory, Leiden University, PO Box 9513, NL-2300 RA Leiden, the Netherlands*

Accepted 2016 April 28. Received 2016 April 28; in original form 2016 February 14

ABSTRACT

Accretion on to central massive black holes in galaxies is often modelled with the Bondi solution. In this paper, we study a generalization of the classical Bondi accretion theory, considering the additional effects of the gravitational potential of the host galaxy, and of electron scattering in the optically thin limit. We provide a general analysis of the bias in the estimates of the Bondi radius and mass accretion rate, when adopting as fiducial values for the density and temperature at infinity the values of these quantities measured at finite distance from the central black hole. We also give general formulae to compute the correction terms of the critical accretion parameter in relevant asymptotic regimes. A full analytical discussion is presented in the case of a Hernquist galaxy, when the problem reduces to the discussion of a cubic equation, therefore, allowing for more than one critical point in the accretion structure. The results are useful for observational works (especially in the case of systems with a low Eddington ratio), as well as for numerical simulations, where accretion rates are usually defined in terms of the gas properties near the black hole.

Key words: galaxies: elliptical and lenticular, cD – galaxies: nuclei – X-rays: galaxies – X-rays: ISM.

1 INTRODUCTION

The Bondi solution of accretion on a point mass (Bondi 1952), due to its inherent simplicity, is a standard tool for the interpretation of observations of the accretion phenomenon, and the starting point for the development of recipes for the mass accretion rate, to be adopted for example in semi-analytical models and numerical simulations that lack the resolution to study gas transport down to parsec scale. In cosmological simulations and semi-analytical models of the early growth of massive black holes (hereafter MBHs), and of the co-evolution of MBHs and their host galaxies, the Bondi accretion rate is used to link the mass supply to the accretion discs surrounding MBHs with the density and temperature of their environment (e.g. Fabian & Rees 1995; Di Matteo, Springel & Hernquist 2005; Volonteri & Rees 2005; Hopkins et al. 2006; Booth & Schaye 2009; Park & Ricotti 2011; Wyithe & Loeb 2012; Hirschmann et al. 2014; Curtis & Sijacki 2015; DeGraf et al. 2015; Inayoshi, Haiman & Ostriker 2016). Another important application of the classical Bondi model is to estimate the mass accretion rate on MBHs at the centre of galaxies, by using observed values of the gas density and temperature in the vicinity of the MBH (e.g. Loewenstein et al. 2001; Baganoff et al. 2003; Pellegrini 2005, 2010; Allen et al. 2006; Rafferty et al. 2006; McNamara, Rohanizadegan & Nulsen 2011; Wong et al. 2014; Russell et al. 2015). In this view, one assumes that these values represent the true boundary conditions (i.e. at infinity) for the Bondi problem (see Quataert & Narayan 2000).

However, it is recognized that even the knowledge of the true boundary conditions would not be enough for a proper treatment of mass accretion on MBHs at the centre of galaxies: first, because the MBH is not isolated, being at the bottom of the host galaxy potential well; secondly, because the radiation emitted by the inflowing material interacts with the material itself, with the consequent establishment of unsteady accretion (for luminosities of the order of $10^{-2}L_{\rm Edd}$ or greater, where $L_{\rm Edd}$ is the Eddington luminosity; e.g. Cowie, Ostriker & Stark 1978); and finally, because the flow also gets mass and energy from the inputs due to stellar evolution (e.g. Ciotti et al. 1991). When the last two of the above circumstances are important, Bondi accretion cannot be applied; during phases of moderate accretion, instead, the problem can be considered almost steady, so that Bondi accretion can be considered a first, reliable approximation of the real situation.

In this paper, we present a quantification of the bias on the estimates of the Bondi radius and mass accretion rate, that is introduced when adopting as boundary values for the density and temperature those at arbitrary but finite distances from the MBHs. First, we derive the exact formulae for this bias, in case of radiation pressure due to electron scattering, and of the additional gravitational potential of a galaxy; we also derive the asymptotic expansion of these formulae close to the MBH. These formulae contain a critical accretion parameter, that in general can be determined only numerically. Then, we present a technique to obtain the analytical expressions

★ E-mail: luca.ciotti@unibo.it

for the critical accretion parameter, in some special cases. A full analytical discussion of the critical points is presented for a Hernquist galaxy model. We finally solve numerically the Bondi problem for an MBH at the centre of a galaxy, and including the effect of radiation pressure due to electron scattering, and compare the numerical results with the analytical ones.

The paper is organized as follows. In Section 2, we recall the main properties of the classical Bondi solution, and we present a preliminary analysis of the mass accretion bias introduced by considering as boundary values for the density and temperature those at points along the solution at finite distance from the MBH. In Section 3, we add to the Bondi solution, in a self-consistent way, the effect of electron scattering, and in Section 4 we consider the full case of the Bondi solution in presence of radiation feedback and a galaxy potential. In Section 5, the particular case of a Hernquist galaxy is presented, building numerically the accretion solution, and also providing a full analytical discussion of the problem. For all these cases, we derive the formulae that allow us to recover the true accretion rate from fiducial estimates of the Bondi radius and accretion rate obtained by assuming classical Bondi accretion. The main conclusions are summarized in Section 6. Finally, three Appendixes contain technical details and relevant formulae useful in analytical and numerical studies.

2 THE CLASSICAL BONDI MODEL

As the present investigation builds on the classical Bondi (1952) accretion model, it is useful to recall its main properties. The classical Bondi theory describes spherically symmetric, steady accretion of a spatially infinite gas distribution on to an isolated central mass, in our case an MBH, of mass $M_{\rm BH}$. The self-gravity, angular momentum and viscosity of the accreting gas, as well as magnetic fields and feedback phenomena, are not considered. The gas is taken to be perfect, and subject to polytropic transformations; thus its pressure (p) and density (ρ) are related by

$$p = \frac{k_{\rm B}\rho T}{\mu m_{\rm p}} = \frac{p_\infty}{\rho_\infty^\gamma}\rho^\gamma, \tag{1}$$

where $1 \leq \gamma \leq 5/3$ is the polytropic index, $m_{\rm p}$ is the proton mass, μ is the mean molecular weight, $k_{\rm B}$ is the Boltzmann constant, and p_∞ and ρ_∞ are, respectively, the gas pressure and the density at infinity. The polytropic gas sound speed is

$$c_{\rm s}^2 = \gamma\frac{p}{\rho}. \tag{2}$$

Note that γ is not necessarily the adiabatic index, so that in the Bondi theory the entropy of the gas can change along the radial streamlines (in fact, polytropic transformations have a constant specific heat, e.g. Chandrasekhar 1939), and in principle, once the solution is known, one could compute the heat balance of each fluid element as it moves towards the MBH.[1]

In spherical symmetry the time-independent continuity equation is

$$4\pi r^2\rho(r)v(r) = \dot{M}_{\rm B}, \tag{3}$$

where $v(r)$ is the gas radial velocity, and $\dot{M}_{\rm B}$ is the time-independent accretion rate on the MBH. The Bernoulli equation, with the appropriate boundary conditions at infinity, becomes

$$\frac{v(r)^2}{2} + \Delta h(r) - \frac{GM_{\rm BH}}{r} = 0, \tag{4}$$

where, from equation (1) and $\gamma > 1$, Δh is given by

$$\Delta h \equiv \int_{p_\infty}^{p}\frac{{\rm d}p}{\rho} = \frac{c_\infty^2}{\gamma-1}\left[\left(\frac{\rho}{\rho_\infty}\right)^{\gamma-1} - 1\right], \tag{5}$$

where c_∞ is the sound speed of the gas at infinity. In the isothermal case, $\gamma = 1$ and $\Delta h = c_\infty^2\ln(\rho/\rho_\infty)$. In the case of an adiabatic transformation, h is the enthalpy per unit mass, while it is just proportional to it for a generic polytropic transformation.

A scalelength of fundamental importance for the problem, the so-called Bondi radius, is naturally defined as[2]

$$r_{\rm B} \equiv \frac{GM_{\rm BH}}{c_\infty^2}. \tag{6}$$

Physically this is the radius at which the gravitational potential energy of a gas element, due to the MBH, is of the order of its thermal energy at infinity. Note that in the following, even when considering more general models, we will use $r_{\rm B}$ as given by the equation above as a length-scale for normalization. Equations (3)–(4) are then recast in dimensionless form by introducing the normalized quantities:

$$x \equiv \frac{r}{r_{\rm B}}, \quad \tilde{\rho} \equiv \frac{\rho}{\rho_\infty}, \quad \tilde{c_{\rm s}} \equiv \frac{c_{\rm s}}{c_\infty} = \tilde{\rho}^{\frac{\gamma-1}{2}}, \tag{7}$$

and the Mach number $\mathcal{M} = v/c_{\rm s}$. For $\gamma > 1$, equations (3)–(4) then become

$$\begin{cases} x^2\mathcal{M}\tilde{\rho}^{\frac{\gamma+1}{2}} = \lambda, \\ \dfrac{\mathcal{M}^2\tilde{c_{\rm s}}^2}{2} + \dfrac{\tilde{\rho}^{\gamma-1}}{\gamma-1} = \dfrac{1}{x} + \dfrac{1}{\gamma-1}, \end{cases} \tag{8}$$

where

$$\lambda \equiv \frac{\dot{M}_{\rm B}}{4\pi r_{\rm B}^2\rho_\infty c_\infty} \tag{9}$$

is the dimensionless accretion parameter: once known, it fixes the accretion rate for assigned $M_{\rm BH}$ and boundary conditions for the accreting gas. Note, how from equations (7)– (8) it follows that all physical quantities can be expressed in terms of the radial profile of the Mach number. By elimination of $\tilde{\rho}$ in equation (8), the Bondi problem reduces to the solution of the equation

$$g(\mathcal{M}) = \Lambda f(x), \qquad \Lambda \equiv \lambda^{\frac{2(1-\gamma)}{\gamma+1}}, \tag{10}$$

where

$$\begin{cases} g(\mathcal{M}) = \mathcal{M}^{\frac{2(1-\gamma)}{\gamma+1}}\left(\dfrac{\mathcal{M}^2}{2} + \dfrac{1}{\gamma-1}\right), \\ f(x) = x^{\frac{4(\gamma-1)}{\gamma+1}}\left(\dfrac{1}{x} + \dfrac{1}{\gamma-1}\right). \end{cases} \tag{11}$$

As well known, Λ cannot be chosen arbitrarily: for $1 < \gamma \leq 5/3$, both $g(\mathcal{M})$ and $f(x)$ have a minimum (that we indicate with $g_{\rm min}$ and $f_{\rm min}$, respectively), thus to satisfy equation (10) $\forall x > 0$ requires

[1] For a polytropic transformation of index γ, adiabatic index $\gamma_{\rm ad}$, and specific heat at constant volume $c_{\rm V}$, the molar specific heat is $c = c_{\rm V}(\gamma_{\rm ad} - \gamma)/(1-\gamma)$. Therefore, when $1 < \gamma < \gamma_{\rm ad}$, a fluid element loses energy as it moves inward and heats.

[2] Sometimes in the literature a factor of 2 appears in the numerator of the definition of the Bondi radius.

that $g_{\rm min} \leq \Lambda f_{\rm min}$, i.e. that $\Lambda \geq \Lambda_{\rm cr} \equiv g_{\rm min}/f_{\rm min}$. Equation (10) then implies

$$\lambda \leq \lambda_{\rm cr} \equiv \left(\frac{f_{\rm min}}{g_{\rm min}}\right)^{\frac{\gamma+1}{2(\gamma-1)}}. \tag{12}$$

It is easy to show that, for $\gamma > 1$:

$$\begin{cases} \mathcal{M}_{\rm min} = 1, \qquad g_{\rm min} = \dfrac{\gamma+1}{2(\gamma-1)}, \\ x_{\rm min} = \dfrac{5-3\gamma}{4}, \quad f_{\rm min} = \dfrac{\gamma+1}{4(\gamma-1)}\left(\dfrac{4}{5-3\gamma}\right)^{\frac{5-3\gamma}{\gamma+1}}, \end{cases} \tag{13}$$

so that for the classical Bondi problem one has

$$\lambda_{\rm cr} = \frac{1}{4}\left(\frac{2}{5-3\gamma}\right)^{\frac{5-3\gamma}{2(\gamma-1)}}. \tag{14}$$

Note that $\lambda_{\rm cr} = e^{3/2}/4$ for $\gamma \to 1^+$, and $\lambda_{\rm cr} = 1/4$ for $\gamma \to 5/3^-$.

In the isothermal case, the analogous of equation (10) is

$$g(\mathcal{M}) + \ln\lambda = f(x), \tag{15}$$

where now

$$\begin{cases} g(\mathcal{M}) = \dfrac{\mathcal{M}^2}{2} - \ln\mathcal{M}, \\ f(x) = \dfrac{1}{x} + 2\ln x. \end{cases} \tag{16}$$

Solutions exist only for $g_{\rm min} + \ln\lambda \leq f_{\rm min}$, i.e. for $\lambda \leq \lambda_{\rm cr} = e^{f_{\rm min}-g_{\rm min}}$. Simple algebra shows that

$$\begin{cases} \mathcal{M}_{\rm min} = 1, \qquad g_{\rm min} = \dfrac{1}{2}, \\ x_{\rm min} = \dfrac{1}{2}, \qquad f_{\rm min} = 2 - 2\ln 2, \end{cases} \tag{17}$$

so that $\lambda_{\rm cr}$ in the isothermal case coincides with the limit of equation (14) for $\gamma \to 1^+$.

In practice, to solve the Bondi problem means to obtain the radial profile of $\mathcal{M}(x)$, for given $\Lambda \geq \Lambda_{\rm cr}$. Unfortunately, equations (10) and (15) do not have an explicit solution, and must be solved numerically. We do not enter in the details of the solutions (see, e.g. Bondi 1952; Frank, King & Raine 1992; Krolik 1998) and, as common in similar studies, we restrict to the critical case $\lambda = \lambda_{\rm cr}$; in this case, $x_{\rm min}$ is also the sonic radius. Among the two critical solutions, we consider that with increasing Mach number approaching the centre. In the following, the function $f(x)$ in equations (11) and (16) is generalized by considering the effect of radiation pressure due to electron scattering, and the additional gravitational field of the host galaxy. In those more general cases, we provide the formulae for the true mass accretion rate, together with its estimates obtained using values of density and temperature at any radius r along the (new) solution, while assuming classical Bondi accretion. The critical solutions for each case are constructed with the aid of a numerical code built on purpose: we first determined numerically the position and the value of the absolute minimum of f (Sections 4 and 5), and, after having determined $\lambda_{\rm cr}$, we evaluated the solution over the whole radial range.

2.1 Mass accretion bias: concepts

Here, we introduce the general procedure that will be considered in the next sections to estimate the Bondi radius and mass accretion rate, for the basic case of the classical Bondi solution. To keep the notation simple, in the following we use the symbol λ to indicate the critical value $\lambda_{\rm cr}$. Later, we will use the same procedure after having included in the problem the effects of radiation pressure due to electron scattering (Section 3), and of the gravitational potential of the host galaxy (Sections 4 and 5).

For assigned values of ρ_∞, T_∞, γ, and $M_{\rm BH}$, the classical Bondi accretion rate is given by equation (9):

$$\dot{M}_{\rm B} = 4\pi r_{\rm B}^2 \lambda \rho_\infty c_\infty. \tag{18}$$

In practice, when dealing with observations or numerical simulations, one inserts in equation (18) the values of ρ and T at a finite distance r from the MBH, and considers them as 'proxies' for ρ_∞ and T_∞. This procedure gives an *estimated* value of the Bondi radius (that we call $r_{\rm e}$) and mass accretion rate (that we call $\dot{M}_{\rm e}$). Here, we investigate how much these $r_{\rm e}$ and $\dot{M}_{\rm e}$ depart from the true values $r_{\rm B}$ and $\dot{M}_{\rm B}$, as a function of r, under the assumption that the Bondi solution holds at all radii.

The fiducial Bondi radius and mass accretion rate are then defined as

$$r_{\rm e}(r) \equiv \frac{GM_{\rm BH}}{c_{\rm s}^2(r)}, \qquad \dot{M}_{\rm e}(r) \equiv 4\pi r_{\rm e}^2(r)\lambda\rho(r)c_{\rm s}(r). \tag{19}$$

In particular, $r_{\rm e}$ can be conveniently normalized to $r_{\rm B}$ as

$$\frac{r_{\rm e}(x)}{r_{\rm B}} = \tilde{c}_{\rm s}(x)^{-2} = \tilde{\rho}(x)^{1-\gamma} = \left(\frac{x^2\mathcal{M}}{\lambda}\right)^{\frac{2(\gamma-1)}{\gamma+1}}, \tag{20}$$

and, from equations (18)– (19) for $\gamma > 1$, the ratio $\dot{M}_{\rm e}/\dot{M}_{\rm B}$ can be expressed in terms of $r_{\rm e}/r_{\rm B}$, independently of the boundary conditions ρ_∞ and T_∞, as

$$\frac{\dot{M}_{\rm e}(x)}{\dot{M}_{\rm B}} = \left[\frac{r_{\rm B}}{r_{\rm e}(x)}\right]^{\frac{5-3\gamma}{2(\gamma-1)}}. \tag{21}$$

Obviously, for $x \to \infty$, one has $r_{\rm e} \to r_{\rm B}$, by definition of $r_{\rm B}$ and $r_{\rm e}$ [equations (6) and (19)]; or, equivalently, because $\tilde{\rho} \to 1$; in turn, one also has that $\dot{M}_{\rm e} \to \dot{M}_{\rm B}$. Note also how, for $\gamma > 1$, $r_{\rm e}$ is always smaller than $r_{\rm B}$, since the gas sound speed increases inward; for $\gamma = 1$, the sound speed is constant, and then $r_{\rm e} = r_{\rm B}$, independently of the distance from the centre.

For the mass accretion rate, in the monoatomic adiabatic case ($\gamma = 5/3$), $\dot{M}_{\rm e}(x) = \dot{M}_{\rm B}$, independently of the distance from the centre, i.e. there is no bias in the estimated mass accretion rate. For $\gamma = 1$, instead, by using equation (20), it can be proved that the bias is just given by $\tilde{\rho}(x)$ at the radius r where the measure is taken, i.e. $\dot{M}_{\rm e}(x) = \tilde{\rho}(x)\dot{M}_{\rm B}$.

A more quantitative insight in the behaviour of equations (20)–(21) is derived from the asymptotic expansion of $\mathcal{M}(x)$ near the centre, which is obtained after computing the expansion of $f(x)$ for $x \to 0$, and of g for $\mathcal{M} \to \infty$, in equations (11) and (16). For $1 \leq \gamma \leq 5/3$, near the centre $\mathcal{M} \propto x^{-\frac{5-3\gamma}{4}}$, and the leading terms of equations (20)–(21) read:

$$\frac{r_{\rm e}(x)}{r_{\rm B}} \sim \left(\frac{\sqrt{2}}{\lambda}\right)^{\gamma-1} x^{\frac{3(\gamma-1)}{2}}, \quad x \to 0^+, \tag{22}$$

$$\frac{\dot{M}_{\rm e}(x)}{\dot{M}_{\rm B}} \sim \left(\frac{\lambda}{\sqrt{2}}\right)^{\frac{5-3\gamma}{2}} x^{-\frac{3(5-3\gamma)}{4}}, \quad x \to 0^+. \tag{23}$$

For $\gamma > 1$, equation (22) confirms that $r_{\rm e}/r_{\rm B}$ decreases as r approaches the centre. For $\gamma = 5/3$ ($\lambda = 1/4$), there is an interesting result: $r_{\rm e} \sim 2^{5/3} r$, i.e. independently of the position r at which the

temperature to derive r_e is taken, it is always concluded that the fiducial Bondi radius is placed at a larger radius ($r_e > r$), and by the same factor.

For what is concerning the mass accretion rate $\dot{M}_e$, from equation (23) one has that $\dot{M}_e(x)/\dot{M}_B \propto x^{-3/2}$, if $\gamma = 1$; thus, $\dot{M}_e$ significantly overestimates $\dot{M}_B$ for $x \to 0$, more than for any other larger γ. Note that in equation (22) it is possible to express r_e/r_B in terms of r/r_e, and then in equation (21) to obtain $\dot{M}_B$ in terms of $\dot{M}_e$ and r/r_e. In this way, the true $\dot{M}_B$ can be recovered from densities and temperatures taken at some (small) distance r from the centre, as $\dot{M}_B \sim (\sqrt{2}/\lambda)(r/r_e)^{3/2}\dot{M}_e(r)$. This represents a useful result for observational and numerical studies, affected by instrumental or grid resolution.

The properties above, together with the trend of $r_e(x)/r_B$ with x for different γ, are illustrated by Fig. 1, that uses the numerical results of our code. The figure shows how r_e is smaller than r_B, and how this underestimate increases with r decreasing, and for increasing γ. The lower panel of Fig. 1 shows the trend of $\dot{M}_e(x)/\dot{M}_B$ with x, for different γ; one sees that the use in equation (19) of $\rho(r)$ instead of ρ_∞, of $c_s(r)$ instead of c_∞, and of r_e instead of r_B, leads to an overestimate of the true accretion rate $\dot{M}_B$ (except for $\gamma = 5/3$). For $r < r_B$, the overestimate of $\dot{M}_B$ is significant. The numerical results in Fig. 1, for $x \lesssim 0.1$, are in excellent agreement with those provided by the analytical asymptotic expansions near the centre in equations (22)–(23) [not shown in this figure for clarity; but see the following Fig. 2].

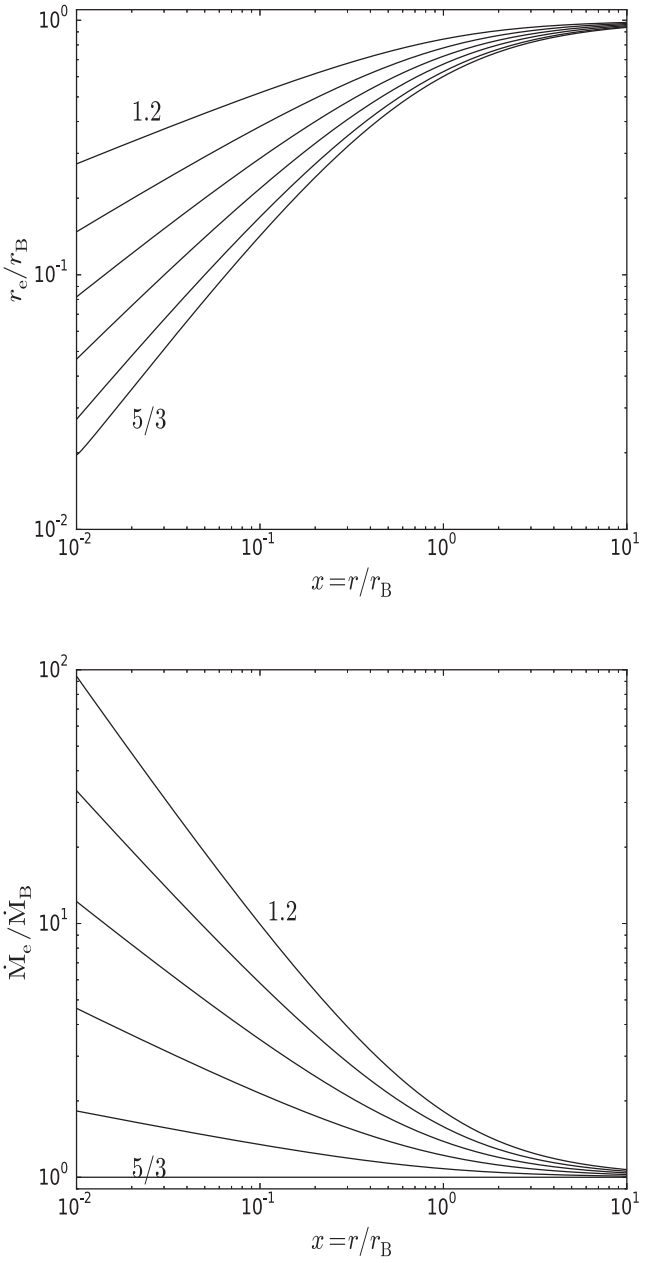

Figure 1. Classical Bondi accretion model. Upper panel: estimated value of the Bondi radius r_e [equation (20)], obtained from T measured at a distance r from the MBH, as a function of r. Lower panel: estimated accretion rate $\dot{M}_e$ in units of the true accretion rate $\dot{M}_B$ [equation (21)], as a function of r. In both panels the polytropic index γ is 1.2, 1.3, 1.4, 1.5, 1.6, 5/3.

3 ADDING THE EFFECTS OF ELECTRON SCATTERING

As well known, the Bondi solution is a purely hydrodynamical flow, where heat exchanges are implicitly described by the polytropic index. Therefore, for given polytropic index, and in absence of shock waves (as for example in the transition from subsonic to supersonic regime for the subcritical $\lambda < \lambda_{cr}$ case), one could follow the entropy evolution of each fluid element along the radial streamline, and determine the reversible heat exchanges. However, in real accretion the energetics can be dominated by the irreversible emission of energy near the MBH, that, for the radiative component, is usually expressed as

$$L = \varepsilon \dot{M}_{acc} c^2, \tag{24}$$

where ε is the efficiency of the release of the accretion energy, and $\dot{M}_{acc}$ is the mass accretion rate; in the classical Bondi accretion, $\dot{M}_{acc} = \dot{M}_B$. In principle ε can depend on luminosity L or on $\dot{M}_{acc}$ [especially at low luminosities, as in the advection dominated accretion flow family (Narayan & Yi 1995), and its variants]. At high accretion rates, the efficiency is of the order of $\varepsilon_0 = 0.1$, and the accretion is likely unsteady, so that Bondi accretion cannot be used (e.g. Ciotti & Ostriker 2012, for a review). The emitted radiation interacts with the surrounding medium and modifies the accretion process: the radiation effects can be sufficiently strong to stop accretion (the so-called negative feedback), and shut-off the central active galactic nucleus. Stationarity is almost impossible in these circumstances (Binney & Tabor 1995; Ciotti & Ostriker 1997, 2001; Park et al. 2014).

However, when restricting to low accretion rates and considering only electron scattering, in the optically thin regime it is possible to generalize the classical Bondi accretion solution by taking into account the radiation pressure effect (Taam, Fu & Fryxell 1991; Fukue 2001; Lusso & Ciotti 2011). In fact, for electron scattering in the optically thin regime and in spherical symmetry, the effective force experienced by a gas element can be written as

$$F(r) = -\frac{GM_{BH}\rho(r)\chi}{r^2}, \quad \chi \equiv 1 - l, \quad l \equiv \frac{L}{L_{Edd}}, \tag{25}$$

where $L_{Edd} = 4\pi c G M_{BH} m_p/\sigma_T$ is the Eddington luminosity, and $\sigma_T = 6.65 \times 10^{-25}\mathrm{cm}^2$ is the Thomson cross-section. In the optically thin regime, being l independent of radius, the radiation feedback can be implemented in equation (11) as a correction that

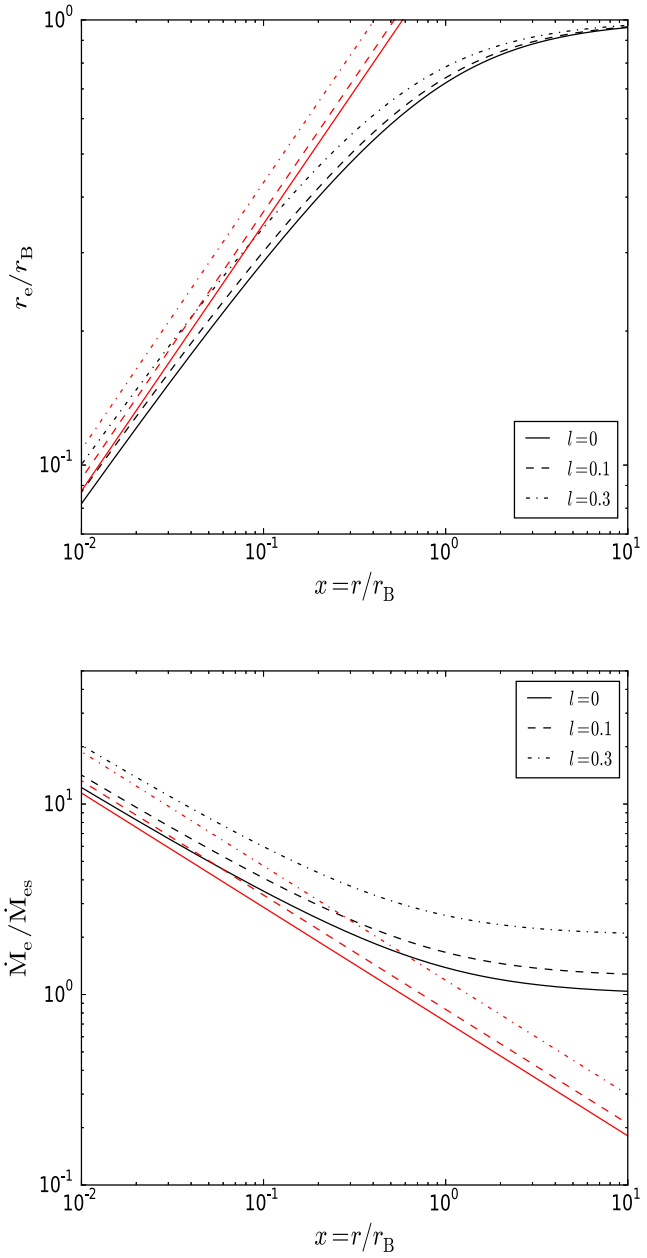

Figure 2. Bondi accretion model with electron scattering, for three values of $l = L/L_{\rm Edd}$ indicated in the panels. Upper panel: estimated Bondi radius $r_{\rm e}$ [equation (33)], obtained from T measured at a distance r from the MBH, as a function of r. Lower panel: the estimated accretion rate $\dot{M}_{\rm e}$, in units of the true accretion rate, according to the Bondi theory, that includes electron scattering $\dot{M}_{\rm es}$ [equation (34)], as a function of r. In both panels the black lines show the numerical solutions corresponding to different values of the normalized accretion luminosity, and the red ones the asymptotic solutions provided by equations (35)–(36); $\gamma = 1.4$.

reduces the gravitational force of the MBH by the factor χ; thus, for $\gamma > 1$, the function f in equation (11) becomes

$$f(x) = x^{\frac{4(\gamma-1)}{\gamma+1}} \left(\frac{\chi}{x} + \frac{1}{\gamma - 1} \right). \tag{26}$$

We do not give the analogous formula for the isothermal case [equation (16)], because, as in the classical case, the relevant quantities can be obtained by taking the limit for $\gamma \to 1^+$ of the formulae in the general polytropic case. One can repeat step by step the analysis of Section 2, and show that the (unique) minimum of f in equation (26) is reached for

$$x_{\rm min} = \frac{\chi(5 - 3\gamma)}{4}. \tag{27}$$

Being $\chi < 1$, the position of the minimum moves inward with respect to the classical case in equation (13), and the value of $f_{\rm min}$ is just that of the classical Bondi accretion [equation (13)] reduced by the factor $\chi^{4(\gamma-1)/(\gamma+1)}$. Since the minimum of $g(\mathcal{M})$ is independent of electron scattering, the critical value of the new accretion parameter $\lambda_{\rm es}$, at a given γ, is

$$\lambda_{\rm es} = \chi^2 \lambda, \tag{28}$$

where λ is the critical parameter in the corresponding classical case. Being $\chi < 1$, $\lambda_{\rm es}$ is lower than in the classical model. The true accretion rate, that we now call $\dot{M}_{\rm es}$, is also reduced with respect to the classical value $\dot{M}_{\rm B}$, for given $M_{\rm BH}$, γ, and boundary conditions at infinity:

$$\dot{M}_{\rm es} = 4\pi r_{\rm B}^2 \lambda_{\rm es} \rho_\infty c_\infty = \chi^2 \dot{M}_{\rm B}. \tag{29}$$

Note that $\dot{M}_{\rm es}$ enters the value of χ through the accretion luminosity L, so that equation (29) can be seen as an implicit equation for $\dot{M}_{\rm es}$. Remarkably, this equation can be explicitly solved by introducing the Eddington mass accretion rate

$$\dot{M}_{\rm Edd} \equiv \frac{L_{\rm Edd}}{\varepsilon_0 c^2}, \quad l = \frac{\dot{M}_{\rm es}}{\dot{M}_{\rm Edd}} \frac{\varepsilon}{\varepsilon_0}. \tag{30}$$

In general ε depends on the accretion rate, but in the following for illustrative purposes we assume $\varepsilon = \varepsilon_0$. From equations (29)–(30), one obtains explicitly $\dot{M}_{\rm es}/\dot{M}_{\rm Edd}$ in terms of $\dot{M}_{\rm B}/\dot{M}_{\rm Edd}$, by solving the quadratic equation:

$$\dot{M}_{\rm es} = \left(1 - \frac{\dot{M}_{\rm es}}{\dot{M}_{\rm Edd}} \right)^2 \dot{M}_{\rm B} \tag{31}$$

(see Lusso & Ciotti 2011). For example, at low accretion rates $\dot{M}_{\rm es} \sim \dot{M}_{\rm B}$, while when $\dot{M}_{\rm B}$ would diverge to infinity, one reaches the asymptotic accretion rate

$$\frac{\dot{M}_{\rm es}}{\dot{M}_{\rm Edd}} \sim 1 - \sqrt{\frac{\dot{M}_{\rm Edd}}{\dot{M}_{\rm B}}}. \tag{32}$$

We now apply to the Bondi solution with electron scattering the same procedure of Section 2.1, to quantify the differences, as a function of radius, between the true ($r_{\rm B}$) and estimated ($r_{\rm e}$) Bondi radius, and the true ($\dot{M}_{\rm es}$) and estimated ($\dot{M}_{\rm e}$) accretion rate, where $r_{\rm e}$ and $\dot{M}_{\rm e}$ are defined as in equation (19). It is easy to show that

$$\frac{r_{\rm e}(x)}{r_{\rm B}} = \tilde{c}_{\rm s}(x)^{-2} = \tilde{\rho}(x)^{1-\gamma} = \left(\frac{x^2 \mathcal{M}}{\lambda_{\rm es}} \right)^{\frac{2(\gamma-1)}{\gamma+1}}, \tag{33}$$

$$\frac{\dot{M}_{\rm e}(x)}{\dot{M}_{\rm es}} = \frac{\lambda}{\lambda_{\rm es}} \left[\frac{r_{\rm B}}{r_{\rm e}(x)} \right]^{\frac{5-3\gamma}{2(\gamma-1)}} = \frac{1}{\chi^2} \left[\frac{r_{\rm B}}{r_{\rm e}(x)} \right]^{\frac{5-3\gamma}{2(\gamma-1)}}, \tag{34}$$

where the density and temperature profiles are now those appropriate for accretion with electron scattering. For $x \to \infty$, by definition, $r_{\rm e} \to r_{\rm B}$. Again, as for the classical Bondi problem in Section 2.1, $r_{\rm e}$ is always smaller than $r_{\rm B}$ for $\gamma > 1$, since the gas sound speed increases inward;[3] for $\gamma = 1$, $r_{\rm e} = r_{\rm B}$ independently of the distance r from the centre.

[3] This trend for the radial behaviour of T is easily understood when considering that the problem with electron scattering is just the classical Bondi problem on an MBH of reduced mass equal to $\chi M_{\rm BH}$.

For the mass accretion rate, again in analogy with what found for the classical Bondi problem, we have that $\dot{M}_e(x) \to \dot{M}_{es}/\chi^2 = \dot{M}_B$ for $x \to \infty$; that, for $\gamma = 5/3$, $\dot{M}_e(x) = \dot{M}_{es}/\chi^2$ independent of r; and that, for $\gamma = 1$, $\dot{M}_e(x) = \tilde{\rho}(x)\dot{M}_{es}/\chi^2 = \tilde{\rho}(x)\dot{M}_B$. Note that now the resulting bias depends not only on the distance r where the density and temperature are taken, but also on the value of $\dot{M}_{es}/\dot{M}_{Edd}$, through the parameter χ.

The asymptotic analysis shows that near the centre:

$$\frac{r_e(x)}{r_B} \sim \chi^{\frac{3(1-\gamma)}{2}} \left(\frac{\sqrt{2}}{\lambda}\right)^{\gamma-1} x^{\frac{3(\gamma-1)}{2}}, \quad x \to 0^+, \tag{35}$$

$$\frac{\dot{M}_e(x)}{\dot{M}_{es}} \sim \chi^{\frac{7-9\gamma}{4}} \left(\frac{\lambda}{\sqrt{2}}\right)^{\frac{5-3\gamma}{2}} x^{-\frac{3(5-3\gamma)}{4}}, \quad x \to 0^+. \tag{36}$$

In particular, the right-hand side in equations (35)–(36) are just the right hand side of equations (22)–(23) for the classical Bondi problem, multiplied by $\chi^{\frac{3(1-\gamma)}{2}}$ and $\chi^{\frac{7-9\gamma}{4}}$, respectively. Therefore, r_e/r_B again decreases for $\gamma > 1$ and $x \to 0$. For $\gamma = 5/3$, r_e scales linearly with r, as $r_e \sim 2^{5/3} r/\chi$, and again $r_e > r$, but by a larger factor than in classical Bondi accretion. For $\gamma < 5/3$, $\dot{M}_e$ overestimates the true accretion rate $\dot{M}_{es}$; for $\gamma = 1$, $\dot{M}_e \propto x^{-3/2}$. Again, as in the classical Bondi problem, it is possible to recover the true accretion rate from r_e and $\dot{M}_e$ near the centre, as $\dot{M}_{es} \sim \sqrt{\chi}(\sqrt{2}/\lambda)(r/r_e)^{3/2}\dot{M}_e(r)$. The resulting quadratic equation for $\dot{M}_{es}$ can be easily solved after writing the correction coefficient χ in terms of $\dot{M}_{es}$, following the procedure described below equation (30).

The properties above are illustrated by Fig. 2, that shows the numerical and asymptotic solutions for r_e/r_B [equations (33) and (35)], and for $\dot{M}_e/\dot{M}_{es}$ [equations (34) and (36)], as a function of the distance r, for different values of l, and γ fixed to the representative value 1.4. The figure gives a quantification of the bias on the estimates of the Bondi radius and mass accretion rate: r_e is always an underestimate of r_B, as expected, while $\dot{M}_e$ is always an overestimate of the true accretion rate, even by a large factor if $r < 0.1 r_B$ (and, of course, increasing for larger l).

4 BONDI ACCRETION WITH ELECTRON SCATTERING ON TO MBHs AT THE CENTRE OF GALAXIES

We can now discuss the full problem, i.e. we investigate how standard Bondi accretion is modified by the additional potential of the host galaxy, and by electron scattering. We then generalize the previous conclusions about the fiducial Bondi radius r_e and mass accretion rate $\dot{M}_e$ obtained using quantities at finite distance from the MBH.

We assume spherical symmetry for the host galaxy, so that its gravitational potential can be written in full generality as

$$\phi_g = -\frac{GM_g}{r_g}\,\psi\left(\frac{r}{r_g}\right), \tag{37}$$

where M_g, r_g and ψ are, respectively, the total galaxy mass, a characteristic scalelength, and the dimensionless galaxy potential. By introducing the parameters

$$\mathcal{R} \equiv \frac{M_g}{M_{BH}}, \quad \xi \equiv \frac{r_g}{r_B}, \tag{38}$$

the effective total gravitational potential to be inserted in the expression for the function f can be written as

$$\phi_t = -\frac{GM_{BH}}{r_B}\left[\frac{\chi}{x} + \frac{\mathcal{R}}{\xi}\,\psi\left(\frac{x}{\xi}\right)\right]. \tag{39}$$

The addition of the galaxy potential ϕ_g changes the function f in equations (11) and (16), and consequently also the values of $f_{min}(\chi, \mathcal{R}, \xi)$ and of the critical λ (that now we call λ_t); the function $g(\mathcal{M})$ is unaffected by the addition of the galaxy. Thus, λ_t is now given in the polytropic case by equation (12) with the new value of f_{min}, and again the isothermal case can be obtained as a limit for $\gamma \to 1^+$ of the polytropic problem. For a generic galaxy model, it is no longer possible to obtain an analytical expression for x_{min}, f_{min}, and λ_t, and they must be determined numerically. As we will see in Section 5, the galaxy potential can produce more than one minimum for the function f; in this case it is easy to conclude that the general considerations after equations (11) and (16) refer to the *absolute* minimum of f, and so x_{min} gives – along the critical solution – the location of the *sonic point*.[4] Of course, when $\mathcal{R} \to 0$ (or $\xi \to \infty$), the galaxy contribution vanishes, $\lambda_t = \lambda_{es}$, and the formulae of Section 3 hold. Instead, by setting $\chi = 1$, one can determine the sole gravitational effects of the host galaxy. In Appendix A, we describe how to compute the correction terms for λ due to the presence of a generic galaxy model, in some special cases, while in Appendix B an important property of monoatomic adiabatic accretion in generic galaxy potentials is derived, i.e. that $\lambda_t = \lambda_{es} = \chi^2/4$, where the last identity comes from equation (28) with $\gamma = 5/3$.

4.1 Mass accretion estimates

Following the procedure described in Sections 2 and 3, we evaluate the deviation of r_e and $\dot{M}_e$ from the true values of r_B and of the mass accretion rate, that we now indicate as $\dot{M}_t$. The presence of a galaxy changes the accretion rate on the central MBH; equation (9) still holds, but now

$$\dot{M}_t = 4\pi r_B^2 \lambda_t \rho_\infty c_\infty = \frac{\lambda_t}{\lambda}\dot{M}_B, \tag{40}$$

where $\dot{M}_B$ is the Bondi accretion rate, for the same chosen boundary conditions ρ_∞ and c_∞, in absence of the galaxy and of radiation pressure. The expressions for r_e and $\dot{M}_e$ are given by the analogous of equations (20)–(21) and (33)–(34), where now the physical variables are taken along the solution in presence of the galaxy and of electron scattering. From equation (19), then one has

$$\frac{r_e(x)}{r_B} = \tilde{c}_s(x)^{-2} = \tilde{\rho}(x)^{1-\gamma} = \left(\frac{x^2\mathcal{M}}{\lambda_t}\right)^{\frac{2(\gamma-1)}{\gamma+1}}, \tag{41}$$

and

$$\frac{\dot{M}_e(x)}{\dot{M}_t} = \frac{\lambda}{\lambda_t}\left[\frac{r_B}{r_e(x)}\right]^{\frac{5-3\gamma}{2(\gamma-1)}}. \tag{42}$$

For $x \to \infty$, by definition, $r_e \to r_B$, and, $\dot{M}_e(x) \to \dot{M}_t\lambda/\lambda_t = \dot{M}_B$. As in the previous simpler accretion cases, for $\gamma = 1$ one has that $r_e = r_B$, independently of the distance from the centre, and $\dot{M}_e(x) = \tilde{\rho}(x)\dot{M}_t\lambda/\lambda_t = \tilde{\rho}(x)\dot{M}_B$. For $\gamma = 5/3$, $\lambda_t = \chi^2/4$ (Appendix B), and so $\dot{M}_t = \dot{M}_{es}$ and $\dot{M}_e(x) = \dot{M}_t/\chi^2$, independent of r, and also independent of the presence of the galaxy. Of course the bias does not depend on r, but depends on χ, and then in general it is still present. Additional properties of λ_t are discussed in the next section. Section 5.2 shows the radial dependence of $\dot{M}_e(x)/\dot{M}_t$ in the particular case of a Hernquist galaxy, for different γ and χ values.

[4] It can be shown (e.g. Frank et al. 1992) that the sonic radius r_s obeys the identity $c_s^2(r) = (r/2)\,\mathrm{d}\phi_t/\mathrm{d}r$ where ϕ_t is the total gravitational potential.

Repeating the asymptotic analysis of Sections 2 and 3, near the centre we now derive

$$\frac{r_{\rm e}(x)}{r_{\rm B}} \sim \chi^{\frac{\gamma-1}{2}} \left(\frac{\sqrt{2}}{\lambda_{\rm t}}\right)^{\gamma-1} x^{\frac{3(\gamma-1)}{2}}, \quad x \to 0^+, \tag{43}$$

$$\frac{\dot{M}_{\rm e}(x)}{\dot{M}_{\rm t}} \sim \chi^{-\frac{5-3\gamma}{4}} \frac{\lambda}{\sqrt{2}} \left(\frac{\sqrt{2}}{\lambda_{\rm t}}\right)^{\frac{3(\gamma-1)}{2}} x^{-\frac{3(5-3\gamma)}{4}}, \quad x \to 0^+. \tag{44}$$

As in the other cases, $r_{\rm e}/r_{\rm B}$ decreases for $\gamma > 1$ and $x \to 0$. For $\gamma = 5/3$, $r_{\rm e}$ scales linearly with r, as $r_{\rm e} \sim 2^{5/3} r/\chi$ (because, for $\gamma = 5/3$, $\lambda_{\rm t} = \lambda_{\rm es} = \chi^2/4$, see Appendix B), and again $r_{\rm e} > r$ for $r \to 0$, but by a larger factor than in classical Bondi accretion. Remarkably, near the centre it is again possible to obtain the true $\dot{M}_{\rm t}$ by using the fiducial $\dot{M}_{\rm e}$ and $r_{\rm e}$. In fact, for $x \to 0$, $\lambda_{\rm t}$ cancels out from equations (42)–(43), and $\dot{M}_{\rm t} \sim \sqrt{\chi}(\sqrt{2}/\lambda)(r/r_{\rm e})^{3/2}\dot{M}_{\rm e}(r)$. This quadratic equation can be easily solved for $\dot{M}_{\rm t}$ as in Section 3, after expressing the radiative correction coefficient χ in term of $\dot{M}_{\rm t}$, following the procedure described below equation (30).

Before proceeding with the solution of this accretion problem, we need to examine whether $L_{\rm Edd}$ changes in presence of a galaxy. If this is the case, then the dimensionless accretion luminosity $l = L/L_{\rm Edd}$ and the associated χ would be a function of the specific model investigated. However, it can be shown that for any given galaxy model, characterized by the cumulative mass distribution $M_{\rm g}(r)$, the Eddington luminosity depends on radius as

$$L_{\rm Edd}(r) = \left[1 + \frac{M_{\rm g}(r)}{M_{\rm BH}}\right] L_{\rm Edd}, \tag{45}$$

where $L_{\rm Edd}$ is the classical value whose expression is given below equation (25). Therefore, $L_{\rm Edd}(r)$ is minimum at the centre, with $L_{\rm Edd}(0) = L_{\rm Edd}$, and steady accretion – also in presence of a galaxy – cannot exist for $L > L_{\rm Edd}$. This implies that l and χ, also in presence of a galaxy, are still defined as in Section 4.

5 THE CASE OF A HERNQUIST GALAXY MODEL

In order to provide quantitative estimates for the trends of $r_{\rm e}(x)/r_{\rm B}$ and $\dot{M}_{\rm e}(x)/\dot{M}_{\rm t}$, we need to adopt a specific galaxy model, to determine $\lambda_{\rm t}$. As already noticed, the value of $\lambda_{\rm t}$ is known once the absolute minimum $f_{\rm min}(\chi, \mathcal{R}, \xi)$ is known; this, in turn, requires the determination of $x_{\rm min}$. As a realistic galactic potential, we consider that corresponding to the Hernquist (1990) density profile that describes well the mass distribution of early-type galaxies; however, we stress that several results below remain true also for other galaxy models, such as the so-called γ-models (Dehnen 1993; Tremaine et al. 1994). The Hernquist model with a central MBH has been recently adopted for a numerical investigation of the bulge-driven, Bondi fuelling of seed black holes (Park et al. 2016); our analysis below nicely reinforces their conclusions, and provides analytical explanations for some of the scalings they find (see also Appendix C). The gravitational potential of the Hernquist model is

$$\phi_{\rm g} = -\frac{GM_{\rm g}}{r + r_{\rm g}}, \tag{46}$$

where the scalelength $r_{\rm g}$ is related to the galaxy effective radius $R_{\rm e}$ as $r_{\rm g} \simeq R_{\rm e}/1.82$. Thus, from equation (39) for $\gamma > 1$ one has

$$f(x) = x^{\frac{4(\gamma-1)}{\gamma+1}} \left(\frac{\chi}{x} + \frac{\mathcal{R}}{x+\xi} + \frac{1}{\gamma-1}\right), \tag{47}$$

and the formula for the isothermal case is obtained from equation (16).

5.1 Analytical results

Before presenting the numerical results for the Hernquist galaxy model, a preliminary discussion is useful in order to obtain hints on the expected behaviour of the solution. For the Hernquist model, the analysis is sufficiently simple to prove some interesting results, yet the case already illustrates the difficulties encountered in accretion problems in galaxy potentials. Basically, the following analysis focuses on the behaviour (number and location) of the critical points of f, on the determination of the absolute minimum $f_{\rm min}$, and finally on the dependence of $\lambda_{\rm t}$ on the model parameters.

The full analysis of the number and location of minima of equation (47) is given in Appendix C, where equation (C1) gives the expression for f' when $\gamma > 1$; for $\gamma = 1$, f' is obtained as the limit for $\gamma \to 1^+$ of the expression for f' in equation (C1).

From the expression for $f(x)$, one sees that in three cases the determination of $x_{\rm min}$ and $f_{\rm min}$ is trivial. The first is when $\xi \to \infty$ (or $\mathcal{R} \to 0$), then the galaxy contribution vanishes, and equations (27)–(28) are recovered. The second case corresponds to $\xi = 0$, when the problem reduces to Bondi accretion on to an MBH of mass $(\chi + \mathcal{R})M_{\rm BH}$. For these two cases, the position of the only minimum of the function f (i.e. of the sonic radius), and the critical value $\lambda_{\rm t}$, for $1 \le \gamma \le 5/3$, are given by

$$x_{\rm min} = \frac{(\chi + \mathcal{R})(5 - 3\gamma)}{4}, \quad \lambda_{\rm t} = (\chi + \mathcal{R})^2 \lambda, \tag{48}$$

where λ is the critical value for the corresponding classical Bondi problem (Section 2). A third simple case is when $\xi \ge 0$ but $\gamma = 5/3$: f' is definite positive [equation (C3)], so that the minimum of f is reached at the centre (as for the adiabatic Bondi problem without the galaxy). Simple algebra shows that the Hernquist model with $\xi > 0$ obeys the (very weak) hypotheses of Appendix B, and so the general identity $\lambda_{\rm t} = \chi^2/4$ holds. Note that this value differs from that in equation (48) pertinent to the $\xi = 0$ case: in fact, in Appendix B we also show that the $\gamma = 5/3$ case for the Hernquist model is singular for $\xi \to 0$, as also manifested by the fact that $\lim_{\xi \to 0} f_{\rm min} = \chi$ while $f_{\rm min}(\xi = 0) = \chi + \mathcal{R}$. As a strictly related result, again from Appendix B, it follows that accretion in the $\gamma = 5/3$ case is impossible in a generic galaxy models without a central MBH, because $f_{\rm min} = 0$ and so $\lambda_{\rm t} = 0$ (as confirmed by setting $\chi = 0$ in the identity above).

As shown in Appendix C, for accretion in the general Hernquist galaxy model with a central MBH and electron scattering, $x_{\rm min}$ can be obtained by solving an algebraic (cubic) equation, thus providing, in principle, the explicit expression for $f_{\rm min}$ and $\lambda_{\rm t}$, at variance with the common situation encountered for other galaxy models. The solution presents no difficulties, however it is quite cumbersome, and here we just recall that, depending on the specific values of $\mathcal{R}$, ξ, and γ, there can be a single minimum for f, or two minima and one maximum. In Appendix C, we provide analytical formulae that can be easily implemented in numerical studies, allowing us to determine, for any given choice of $\mathcal{R}$, ξ, and γ, the number and the location of the critical points of f.

Although the explicit expression for $\lambda_{\rm t}$ can be easily constructed, here we just give some hints on its behaviour by considering cases of perturbative analysis (namely, for $\xi \to \infty$ or $\mathcal{R} \to 0$, and for $\xi \to 0$), along the lines described in Appendix A [equation (A6) and following for details]. For example, for $\gamma = 1$, the results in Appendix C3 show that there is only one critical point for f in the considered cases, and expanding around the unperturbed minimum [whose position is given in equation (27) for $\xi \to \infty$ or $\mathcal{R} \to 0$,

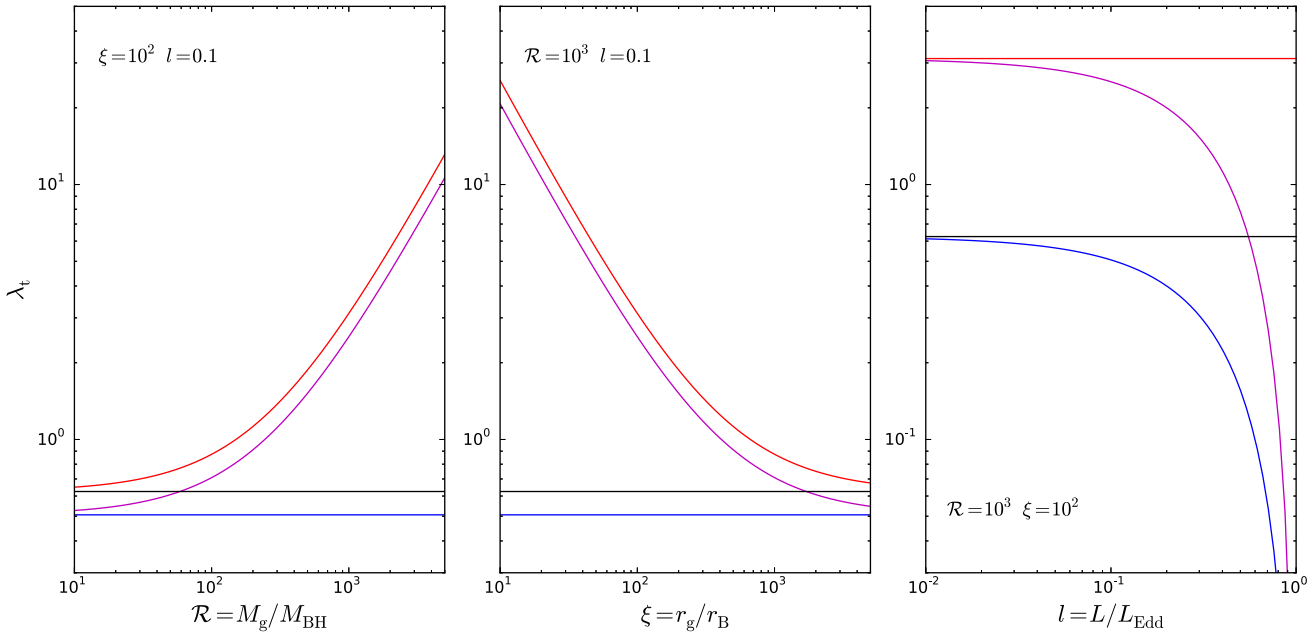

Figure 3. Bondi accretion model with electron scattering at the centre of a Hernquist galaxy for the representative value $\gamma = 1.4$: the magenta line shows λ_t as a function of $\mathcal{R} = M_g/M_{BH}$ (left-hand panel), of $\xi = r_g/r_B$ (middle panel), and of l (right-hand panel). λ_t is also compared to λ of the classical Bondi model (in black), to that of the Bondi model with a Hernquist galaxy and $l = 0$ (in red), and to λ_{es} of the Bondi model with electron scattering (in blue). As expected, $\lambda_{es} < \lambda$, because the electron scattering lowers λ [see equation (28)]; similarly, λ_t is always lower than the red line corresponding to the galaxy only [see also equations (49)–(50)].

and in equation (48) for $\xi \to 0$], one finds that the leading term of λ_t is

$$\lambda_t \sim \lambda \times \begin{cases} \chi^2 e^{\frac{\mathcal{R}}{\xi+\chi/2}}, & \xi \to \infty, \quad \mathcal{R} \to 0, \\ (\chi+\mathcal{R})^2 e^{-\frac{4\mathcal{R}\xi}{(\chi+\mathcal{R})^2}}, & \xi \to 0, \end{cases} \tag{49}$$

where $\lambda = e^{3/2}/4$.

A similar analysis can be performed for $1 < \gamma < 5/3$. A careful expansion around the absolute minimum of f, as determined from Appendix C, shows that for $\xi \to \infty$ (or $\mathcal{R} \to 0$), and for $\xi \to 0$ we have, respectively,

$$\lambda_t \sim \lambda \times \begin{cases} \chi^2 \left[1 + \dfrac{4(\gamma-1)(5-3\gamma)\mathcal{R}}{(\gamma+1)[\chi(5-3\gamma)+4\xi]}\right]^{\frac{\gamma+1}{2(\gamma-1)}}, \\ (\chi+\mathcal{R})^2 \left[1 - \dfrac{16\,\mathcal{R}\,\xi(\gamma-1)}{(1+\mathcal{R})^2(\gamma+1)(5-3\gamma)}\right]^{\frac{\gamma+1}{2(\gamma-1)}}. \end{cases} \tag{50}$$

Note, how equation (50) for $\gamma \to 1$ recovers both cases of equation (49). As expected, however, the second of equation (50) is singular for $\gamma \to 5/3^-$, for the reasons described in Appendix B. Note that, at variance with the Bondi accretion with electron scattering only, now the electron scattering coefficient χ cannot be factorized in the expression for λ_t, i.e. λ_t in general cannot be factorized as equation (28) as the product of the electron-scattering coefficients times a function relative to the galaxy accretion without electron-scattering effects. It follows that in presence of a galaxy the procedure described in Section 4 [equations (31)–(32)] cannot be applied analytically.

We stress that all the formulae above have been also derived by direct expansion of the exact solution of equations (C2), thus providing an independent test of the expansion procedure in Appendix A.

5.2 Numerical results

For a Hernquist galaxy potential, it is not possible to obtain the analytical expression for the critical accretion parameter λ_t; thus, we determined numerically the density and temperature profiles of the Bondi model with electron scattering and a Hernquist galaxy, and calculated λ_t, r_e, and $\dot{M}_e/\dot{M}_t$. The results for λ_t are plotted in Fig. 3, where we show the trend of λ_t with respect to $\mathcal{R} = M_g/M_{BH}$, for fixed $\xi = 100$ and $l = 0.1$, with respect to $\xi = r_g/r_B$ for $\mathcal{R} = 10^3$ and $l = 0.1$, and finally with respect to l for $\mathcal{R} = 10^3$ and $\xi = 100$. In the left-hand panel, for a fixed ξ, for which we assumed a realistic value[5] of 100, λ_t increases as $\mathcal{R}$ increases, i.e. as the galaxy total mass increases. In the middle panel, by setting $\mathcal{R} = 10^3$, as dictated by the Magorrian relation (Magorrian et al. 1998), we see that λ_t decreases as ξ increases, since the effect of the galaxy is vanishing (and in fact λ_t reaches down to λ_{es}). Finally, in the right-hand panel, λ_t goes to zero for increasing values of l. Note that for the adopted, illustrative values of $\mathcal{R}$ and ξ, the analysis in Appendix C3 (see also Fig. C1) shows that there are three critical points for f (two minima and one maximum), so that λ_t is obtained from the absolute minimum.

These results for λ_t are also compared to those obtained for the previous simpler models, i.e. the λ of the classical Bondi model, the lower λ_{es} of the Bondi model with electron scattering, and that of the Bondi model with only the Hernquist galaxy. The latter keeps always larger than λ_t, since the effect of the electron scattering is to lower λ [equation (28)]; of course, it tends to λ of the

[5] When r_B is of the order of few tens of pc, as expected for the MBHs at the centre of early-type galaxies, the value $\xi = 100$ corresponds to r_g of few kpc, i.e. a reasonable value for $r_g \simeq R_e/1.82$.

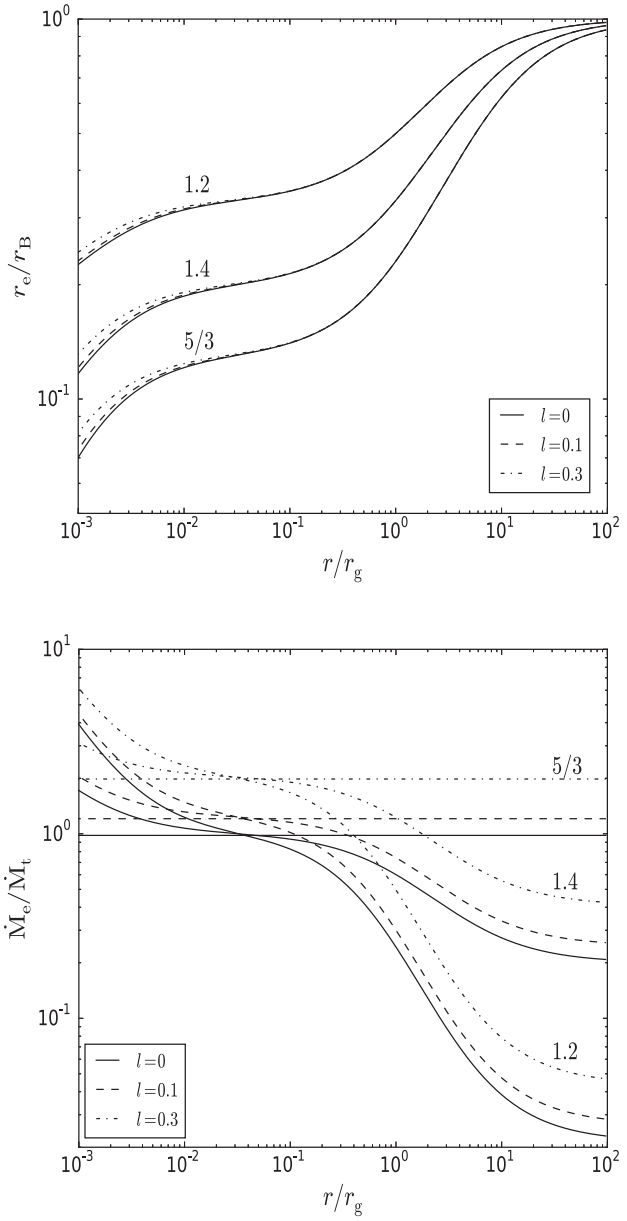

Figure 4. Bondi accretion model with electron scattering at the centre of a Hernquist galaxy. Upper panel: estimated value of the Bondi radius r_e [equation (41)], obtained from T measured at a distance r from the MBH. Lower panel: estimated accretion rate $\dot{M}_e$, in units of the true accretion rate $\dot{M}_t$ [equation (42)], as a function of r. In both panels $l = 0$ (solid line), or $l = 0.1$ (dashed line), or $l = 0.3$ (dotted line); $\mathcal{R} = 10^3$ and $\xi = 100$. Note that, for each l, a different $\dot{M}_t$ is implied, according to equation (40) [see also equation (50) for an explicit dependence of λ_t on l, in a limiting case]. By using equation (11), it can be proved analytically that the coincidence of the abscissa of the intersection points of the curves ($r/r_g \simeq 0.03$ for the chosen model galaxy) is not exact; however, it can be also proved that this almost exact coincidence is a general property of the mass estimator in equation (42).

classical Bondi model for $\mathcal{R} \to 0$ (i.e. for $M_g \to 0$), and for $\xi \to \infty$ (i.e. very large r_g, and then negligible effect of the galaxy). Also, $\lambda_t \to \lambda_{es}$ for $\mathcal{R} \to 0$ and for $\xi \to \infty$ (both cases in which the effect of the galaxy potential is vanishing).

In Fig. 4, we represent r_e and $\dot{M}_e/\dot{M}_t$, as a function of r/r_g, for different values of γ and l. The figure presents a quantification of the bias on the estimates of the Bondi radius and of the true mass accretion rate. Even in this more complex case, r_e provides an underestimate of r_B. For $\gamma = 5/3$, $\dot{M}_e = \dot{M}_t$ if $l = 0$, otherwise $\dot{M}_e$ is always an overestimate of the true accretion rate (increasing for larger l). For the other γs, $\dot{M}_e$ provides an overestimate for $r < r_g$ (more severe for larger l), and an underestimate for $r > r_g$ (less severe for larger l).

6 SUMMARY AND CONCLUSIONS

Due to its simplicity, the classical Bondi accretion theory remains the standard paradigm against which more realistic descriptions are confronted, and observations are interpreted. Also, Bondi accretion is adopted to get a simple approximation for the mass accretion rate in semi-analytical models and numerical simulations, particularly when numerical resolution is not high enough to probe in a self-consistent way the regions near the central MBH. Given the wide use of the classical Bondi theory, and considered that accretion on the MBHs at the centre of galaxies is certainly more complicated than the description provided by this theory, the motivation for this work was to generalize the theory, including the radiation pressure feedback due to electron scattering in the optically thin approximation, and the effect of a general gravitational potential due to a host galaxy. All the hypotheses of classical Bondi accretion (stationarity, absence of rotation, spherical symmetry) were maintained. In addition, this work provides a quantitative answer to a major question, namely what is the bias induced on the estimates of the Bondi radius and mass accretion rate when adopting as bona fide values of the hydrodynamical variables their values at some finite distance from the centre. This issue is relevant for observational (e.g. Pellegrini 2005, 2010; Russell et al. 2015) and numerical works (e.g. Di Matteo et al. 2005; Park et al. 2014; DeGraf et al. 2015). The main results can be summarized as follows.

(1) For the three models of classical Bondi accretion, of accretion with electron scattering, and of accretion on a MBH at the centre of a galaxy with electron scattering, we provide the exact formulae for r_e/r_B (where r_B is fixed for a chosen value of T_∞), as a function of the distance r, the Mach number $\mathcal{M}(r)$, and the accretion parameter; these can be used when the temperature is taken at any r along the 'modified' Bondi solution. We then give the exact formulae for the mass accretion bias (respectively, $\dot{M}_e/\dot{M}_B$, $\dot{M}_e/\dot{M}_{es}$, and $\dot{M}_e/\dot{M}_t$) in terms of the bias on the Bondi radius (r_e/r_B). For a quantitative estimate of the bias, the knowledge of the numerical solution of the associated accretion problem is required.

(2) The formulae above allow us to get some general results without previous knowledge of the exact numerical solution, for particular γ values. In the monoatomic adiabatic case ($\gamma = 5/3$), $\dot{M}_e$ is a constant fraction of the true mass accretion rate ($\dot{M}_B$, or $\dot{M}_{es}$, or $\dot{M}_t$), independently of the distance r from the MBH. The fraction is exactly unity in case of classical accretion ($\dot{M}_e = \dot{M}_B$), and it is given by the ratio of the critical accretion parameters in the other cases: with radiation pressure, $\dot{M}_e = \dot{M}_{es}\lambda/\lambda_{es} = \dot{M}_{es}/\chi^2$; with electron scattering and a galaxy potential, $\dot{M}_e = \dot{M}_t\lambda/\lambda_t = \dot{M}_t/\chi^2$ (see Section 5.1 for more details and the particular case of a Hernquist galaxy). In the isothermal ($\gamma = 1$) case, there is no bias in the estimated value of the Bondi radius ($r_e = r_B$), independently of the distance from the centre; the bias provided by $\dot{M}_e$ is proportional to the density of the accreting material.

(3) The trends of $\dot{M}_e$ and r_e near the centre come from the asymptotic expansion of the solutions for $\mathcal{M}(r)$ and $f(r)$: the bias can be written in terms of the distance r and of the value of the critical

accretion parameter. In particular, for $\gamma > 1$, r_e provides a larger and larger underestimate of r_B as r is approaching the centre [in all cases $r_e/r_B \propto (r/r_B)^{3(\gamma-1)/2}$]. $\dot{M}_e$ correspondingly provides an overestimate of $\dot{M}_B$, $\dot{M}_{es}$, and $\dot{M}_t$.

(4) From the asymptotic expansion of the solutions near the centre, for all the three accretion models considered, it is also shown how to recover the true value of the mass accretion rate from r_e and $\dot{M}_e$ measured at some distance r from the centre. These formulae are useful for observational and numerical works.

(5) When the analytical solution is known for an accretion case, a general asymptotic technique is given that allows to obtain the correction terms for the value of the critical accretion parameter for slightly different models, avoiding the need of a numerical solution of the accretion problem (Appendix A).

(6) In the illustrative case of a Hernquist galaxy model, the determination of x_{min} and λ_t reduces to the study of a cubic equation. The case is fully discussed analytically (Appendix C), and it is shown that more than one critical point for f can exist. We provide a simple analytical framework to determine whether one or two minima occur, and the correction terms for λ_t, determined with the method of point 5).

(7) We finally solved numerically the accretion problem for the three models considered, to provide quantitative estimates of the bias. The analytical formulae turned out to be in perfect agreement with the numerical results.

This work reveals how using values of density and temperature at various radii when deducing accretion properties of MBHs at the centre of galaxies produces values of the mass accretion rate that should be taken with care. We here obtained, however, results sufficiently general to provide correction factors to be used in various observational and numerical works.

ACKNOWLEDGEMENTS

LC is grateful to G. Bertin and J. Ostriker for useful discussions. We thank the anonymous Referee for her/his careful reading of the manuscript. LC and SP were supported by the MIUR grant PRIN 2010-2011, project 'The Chemical and Dynamical Evolution of the Milky Way and Local Group Galaxies', prot. 2010LY5N2T.

REFERENCES

Allen S. W., Dunn R. J. H., Fabian A. C., Taylor G. B., Reynolds C. S., 2006, MNRAS, 372, 21
Baganoff F. K. et al., 2003, ApJ, 591, 891
Binney J., Tabor G., 1995, MNRAS, 276, 663
Binney J., Tremaine S., 1987, Galactic dynamics. Princeton Univ. Press, Princeton, NJ
Bondi H., 1952, MNRAS, 112, 195
Booth C. M., Schaye J., 2009, MNRAS, 398, 53
Chandrasekhar S., 1939, An introduction to the study of Stellar Structure. The University of Chicago press, Dover publications, New York
Ciotti L., D'Ercole A., Pellegrini S., Renzini A., 1991, ApJ, 376, 380
Ciotti L., Ostriker J. P., 1997, APJ, 487, L105
Ciotti L., Ostriker J. P., 2001, ApJ, 551, 131
Ciotti L., Ostriker J. P., 2012, in Kim D.-W., Pellegrini S., eds, Astrophysics and Space Science Library, Vol. 378, Hot Interstellar Matter in Elliptical Galaxies. Springer-Verlag, Berlin, p. 83
Cowie L. L., Ostriker J. P., Stark A. A., 1978, ApJ, 226, 1041
Curtis M., Sijacki D., 2015, MNRAS, 454, 3445
DeGraf C., Di Matteo T., Treu T., Feng Y., Woo J.-H., Park D., 2015, MNRAS, 454, 913
Dehnen W., 1993, MNRAS, 265, 250
Di Matteo T., Springel V., Hernquist L., 2005, Nature, 433, 604
Fabian A. C., Rees M. J., 1995, MNRAS, 277, L55
Frank J., King A., Raine D., 1992, Accretion Power in Astrophysics. Cambridge Univ. Press, Cambridge
Fukue J., 2001, PASJ, 53, 687
Hernquist L., 1990, ApJ, 356, 359
Hirschmann M., Dolag K., Saro A., Bachmann L., Borgani S., Burkert A., 2014, MNRAS, 442, 2304
Hopkins P., Hernquist L., Cox T. J., Di Matteo T., Robertson B., Springel V., 2006, ApJS, 163, 1
Inayoshi K., Haiman Z., Ostriker J. P., 2016, MNRAS, preprint (arXiv:1511.02116)
Krolik J. H., 1998, Active Galactic Nuclei: From the Central Black Hole to the Galactic Environment, Princeton Univ. Press, Princeton, NJ
Loewenstein M., Mushotzky R. F., Angelini L., Arnaud K. A., Quataert E., 2001, ApJ, 555, 21
Lusso E., Ciotti L., 2011, A&A, 525, 115
McNamara B. R., Rohanizadegan M., Nulsen P. E. J., 2011, ApJ, 727, 39
Magorrian J. et al., 1998, AJ, 115, 2285
Narayan R., Yi I., 1995, ApJ, 452, 710
Park K., Ricotti M., 2011, ApJ, 739, 2
Park K., Ricotti M., Di Matteo T., Reynolds C. S., 2014, MNRAS, 445, 2325
Park K., Ricotti M., Natarajan P., Bogdanovic T., Wise J. H., 2016, ApJ, 818, 184
Pellegrini S., 2005, ApJ, 624, 155
Pellegrini S., 2010, ApJ, 717, 640
Quataert E., Narayan R., 2000, ApJ, 528, 236
Rafferty D. A., McNamara B. R., Nulsen P. E. J., Wise M. W., 2006, ApJ, 652, 216
Russell H. R., Fabian A. C., McNamara B., Broderick A. E., 2015, MNRAS, 451, 588
Taam R. E., Fu A., Fryxell B. A., 1991, ApJ, 371, 696
Tremaine S., Richstone D. O., Byun Y.-I., Dressler A., Faber S. M., Grillmair C., Kormendy J., Lauer T. R., 1994, AJ, 107, 634
Volonteri M., Rees M. J., 2005, ApJ, 633, 624
Wong K.-W., Irwin J. A., Shcherbakov R. V., Yukita M., Million E. T., Bregman J. N., 2014, ApJ, 780, 9
Wyithe J. S. B., Loeb A., 2012, MNRAS, 425, 2892

APPENDIX A: ASYMPTOTIC EXPANSION FOR THE ACCRETION PARAMETER

From the discussion in Section 2, it follows that the critical value of the accretion parameter λ in the Bondi theory is given by equation (12). Therefore, λ can be computed explicitly when f_{min} is. For example, this is possible in the classical Bondi problem (also in presence of electron scattering, as shown in Section 3), but in general this is impossible in presence of the galaxy potential. For this reason in order to determine the value of λ, we must resort to numerical evaluation of f_{min}. It is then useful to be able to determine analytically the first correction terms to the value of λ due to the presence of the galaxy. In the following, we present the general procedure for such determination.

The first step is to cast the function $f(x)$ of the problem under scrutiny as the sum of two terms: one (f_0) so that the position of the minimum, x_0, can be explicitly determined, $f_0'(x_0) = 0$. The second term (f_1) is the perturbation term, depending on some small ordering parameter $\epsilon \to 0$. In practice, we suppose we can write

$$f(x) = f_0(x) + f_1(\epsilon, x), \tag{A1}$$

with $f_1(0, x) = 0$. If all the required regularity conditions are satisfied, the position of the new minimum, $x_{min}(\epsilon)$, is given by

$$f'[x_{min}(\epsilon)] = 0, \tag{A2}$$

with

$$x_{\rm min}(\epsilon) = x_0 + \epsilon x_1 + \epsilon^2 x_2 + \cdots \tag{A3}$$

By expansion of equation (A2) and order balance one can in principle determine the perturbation coefficients in equation (A3) at the desired order. For example, provided that $f_0''(x_0) > 0$, it can be proved that

$$x_1 = -\frac{1}{f_0''(x_0)} \left[\frac{\partial^2 f_1}{\partial\epsilon\partial x}\right]_{(\epsilon,x)=(0,x_0)}, \tag{A4}$$

and in such cases when $x_1 = 0$

$$x_2 = -\frac{1}{2f_0''(x_0)} \left[\frac{\partial^3 f_1}{\partial\epsilon^2\partial x}\right]_{(\epsilon,x)=(0,x_0)}. \tag{A5}$$

Once the coefficients are determined, $f_{\rm min}$ is obtained by expansion of equation (A1): for example, in case of a regular perturbation f_1, it is easy to show that at the first order

$$f_{\rm min} \sim f_0(x_0) + \epsilon \left[\frac{\partial f_1(\epsilon, x_0)}{\partial\epsilon}\right]_{\epsilon=0}. \tag{A6}$$

In Section 5, simple perturbation cases are described for the case of a Hernquist galaxy. One is obtained for $\xi \to \infty$, so that $\epsilon = 1/\xi$, the unperturbed problem is the Bondi accretion (with or without electron scattering), with f_0 given in equation (26), and x_0 given by equation (27), while $f_1 = \mathcal{R}\epsilon x^{\frac{4(\gamma-1)}{\gamma+1}}/(1+\epsilon x)$. A second, strictly related case, is that of $\epsilon = \mathcal{R} \to 0$ so that the unperturbed problem is the same as in the previous case, but now $f_1 = \epsilon x^{\frac{4(\gamma-1)}{\gamma+1}}/(\xi + x)$. Finally, we consider $\epsilon = \xi \to 0$. In this case, the galaxy core radius vanishes, so that the unperturbed problem is obtained by considering the Bondi accretion on an MBH of mass $(\chi + \mathcal{R})M_{\rm BH}$, with unperturbed solution x_0 given by equation (48), while $f_1 = -\mathcal{R}\epsilon x^{\frac{4(\gamma-1)}{\gamma+1}}/(\epsilon + x)$.

APPENDIX B: ADIABATIC ACCRETION IN GENERAL POTENTIAL

Here, we show that for $\gamma = 5/3$ the function f' relative to Bondi accretion with electron scattering and in presence of a galaxy, is definite positive for $x \geq 0$, so that f is monotonically increasing and the (only) minimum over the physical domain is attained for $x \to 0$. In fact, for a spherical galaxy model of density profile $\rho_{\rm g}$, finite total mass $M_{\rm g}$, and with a central MBH of mass $M_{\rm BH}$, the total potential in presence of electron scattering can be written as [see equation (39) and Binney & Tremaine (1987)]

$$\phi_{\rm t}(r) = -G\frac{M_{\rm g}(r) + \chi M_{\rm BH}}{r} - 4\pi G\int_r^\infty \rho_{\rm g}(r')r'\,{\rm d}r'. \tag{B1}$$

With the introduction of the dimensionless total potential $\psi_{\rm t} \equiv -r_{\rm B}\phi_{\rm t}/(GM_{\rm BH})$, the general form of equation (47) reads

$$f = x\left(\frac{3}{2} + \psi_{\rm t}\right), \tag{B2}$$

so that

$$f' = \frac{3}{2} + 4\pi\int_x^\infty \tilde{\rho}_{\rm g}(x')x'\,{\rm d}x' > 0, \tag{B3}$$

where $\tilde{\rho}_{\rm g} = r_{\rm B}^3\rho_{\rm g}/M_{\rm BH}$, and this concludes the proof. It follows that for model galaxies with $\lim_{r\to 0} r\phi_{\rm g}(r) = 0$, for $\gamma = 5/3$ one has $f_{\rm min} = \chi$ so that $\lambda_{\rm t} = \lambda_{\rm es} = \chi^2/4$. The Hernquist model with $\xi > 0$ satisfies this hypothesis, but not when $\xi = 0$. This is the reason behind the fact that the $\gamma = 5/3$ case for the Hernquist model is singular, in the sense that the properties of the $\xi = 0$ case cannot be obtained as the limit for $\xi \to 0$, as mentioned in Section 5.1.

Note that for $\gamma < 5/3$, equation (47) shows that the exponent of x in equation (B2) is <1, and the procedure above now confirms that f' can change sign, depending on the specific shape of $\phi_{\rm t}$.

APPENDIX C: ANALYTICAL PROPERTIES OF HERNQUIST CASE

In the general case of Bondi accretion with electron scattering in a Hernquist galaxy with a central MBH and $\xi = r_{\rm g}/r_{\rm B} > 0$ (the case $\xi = 0$ is trivial, as discussed in Section 5), the critical points of f are placed at the zeroes of

$$f' = \frac{4x^{\frac{-2(3-\gamma)}{\gamma+1}}g(x)}{(\gamma+1)(\xi+x)^2}, \tag{C1}$$

where

$$g = x^3 - \frac{(5-3\gamma)(\chi+\mathcal{R}) - 8\xi}{4}x^2 + \frac{\xi\,[2(\gamma-1)\mathcal{R} + 2\xi - (5-3\gamma)\chi]}{2}x - \frac{\xi^2(5-3\gamma)\chi}{4}, \tag{C2}$$

as obtained from equation (47), and $\chi = 1 - L/L_{\rm Edd}$. In the isothermal and in the adiabatic monoatomic cases, this reduces to

$$g = \begin{cases} x^3 - \dfrac{\chi+\mathcal{R}-4\xi}{2}x^2 + \xi(\xi-\chi)x - \dfrac{\xi^2\chi}{2}, \\ x\left[x^2 + 2\xi x + \xi\left(\xi + \dfrac{2\mathcal{R}}{3}\right)\right], \end{cases} \tag{C3}$$

respectively, and in the last case the positivity for $x > 0$ is apparent, in accordance with the general result of Appendix B. Note that in the limiting case of $\chi = 0$, i.e. when formally $L = L_{\rm Edd}$, the problem reduces to Bondi accretion (without electron scattering) in the galaxy potential well only: therefore the obtained formulae can used also to discuss this special class of solutions.

For $1 \leq \gamma < 5/3$, $\xi > 0$ and $\chi > 0$, the constant term in equation (C2) is negative, while the cubic term is positive. This means that f presents always at least one minimum at $x > 0$. However, it may happens that for specific values of the parameters, there are three positive zeros of f, corresponding, for increasing x, to a minimum, a maximum, and a minimum of f, respectively. This is relevant not only for the theoretical implications but also for numerical investigations. In fact, the position of the absolute minimum of f is usually obtained by numerical analysis, and it is of great help to know whether there just one minimum or it is necessary to investigate what of the minima is the absolute one, as required in order to compute the critical accretion parameter λ.

For assigned values of the parameters, the existence and the position of the zeros of f' can be determined by using the Sturm method or from the theory of cubic equations. In fact, after standard reduction of equation (C2) to canonical form $z^3 + pz + q$, one consider the sign of the quantity $R = q^2/4 + p^3/27$. When $R > 0$, the original equation has one real (and so positive) root and two complex conjugate roots. For $R < 0$, there are three real roots, and for $R = 0$ there are a real root and a double (and so real) root. In the case of three real roots, their positivity can be determined from the Descartes' sign rule.

The function R associated with equation (C2) is the product of the factor $\xi^2\mathcal{R}$ times a cubic polynomial that can be ordered as a

function of ξ or $\mathcal{R}$ as

$$\begin{aligned} &64(\gamma+1)\xi^3+4(P_3\mathcal{R}+12P_6)\xi^2\\ &-4\left[P_1\mathcal{R}^2+P_4\mathcal{R}-3(5-3\gamma)\chi P_6\right]\xi\\ &-(5-3\gamma)^2(\chi+\mathcal{R})^2\left[4(\gamma-1)^2\mathcal{R}-P_6\right]\\ &=-4(5-3\gamma)^2(\gamma-1)\mathcal{R}^3-(4P_1\xi+P_2)\mathcal{R}^2\\ &+2(P_3\xi^2-2P_4\xi-P_5)\mathcal{R}+(\gamma+1)\left[4\xi+(5-3\gamma)\chi\right]^3, \end{aligned} \tag{C4}$$

where the coefficients are

$$\begin{cases} P_1=2(\gamma-1)(\gamma^2-30\gamma+33),\\ P_2=(5-3\gamma)^2(11\gamma^2-18\gamma+3)\chi,\\ P_3=2(23\gamma^2+30\gamma-57),\\ P_4=(5-3\gamma)(11\gamma^2-6\gamma+15)\chi,\\ P_5=(5-3\gamma)^2(5\gamma^2-6\gamma-3)\chi^2,\\ P_6=(\gamma+1)(5-3\gamma)\chi. \end{cases} \tag{C5}$$

For assigned values of $\mathcal{R}$, ξ, γ, and χ, is then straightforward to determine numerically the number of real zeros of h by using equations (C4)–(C5), and successively their positivity checking the number of sign variations in the coefficients of equation (C2). In the next sections, we will use equation (C4) to deduce some analytical property of the critical points in some limit case.

C1 Dependence on the galaxy core radius

In terms of ξ, the leading term of equation (C4) is positive, so that $R>0$ for fixed $\mathcal{R}$ and sufficiently large values of ξ, and there is only one minimum for f, as expected from physical considerations. The displacement of the minimum position with respect to equation (27) can be determined by using the method in Appendix A. For very small values of ξ and $5-3\gamma>0$ instead the problem presents three real solutions for $\mathcal{R}>(\gamma+1)(5-3\gamma)\chi/4(\gamma-1)^2$: a careful application of Descartes' rule shows that all the three zeros are positive. In fact, reducing ξ at fixed $\mathcal{R}$, the function f flattens in the outer regions, until $R=0$ and a horizontal flex appears, while the only minimum is placed near the position $x_{\rm min}$ in equation (48): again, the corrective terms can be obtained from Appendix A. Reducing further ξ, the double solution splits, and the minimum–maximum–minimum structure appears. The outer minimum deepens until it becomes the absolute minimum, approaching $x_{\rm min}$ given in equation (48), while the other two zeroes merge at $x=0$. With some work, it is possible to obtain the first terms of the asymptotic expansion for $\xi\to 0$ of the positions of the three critical points of equation (C2), ordered for increasing distance from the origin:

$$\begin{cases} x_1\sim\dfrac{2\mathcal{R}(\gamma-1)-\chi(5-3\gamma)-\sqrt{\Delta}}{(\chi+\mathcal{R})(5-3\gamma)}\xi,\\ x_2\sim\dfrac{2\mathcal{R}(\gamma-1)-\chi(5-3\gamma)+\sqrt{\Delta}}{(\chi+\mathcal{R})(5-3\gamma)}\xi,\\ x_3\sim\dfrac{(\chi+\mathcal{R})(5-3\gamma)}{4}-\dfrac{2\mathcal{R}(3-\gamma)\xi}{(5-3\gamma)(\chi+\mathcal{R})}, \end{cases} \tag{C6}$$

where $\Delta=\mathcal{R}\left[4(\gamma-1)^2\mathcal{R}-P_6\right]$. It is apparent how the reality condition for x_1 and x_2 the first two zeroes matches the reality condition obtained from equation (C4). Moreover, again with some work from equation (C4), it can be proved that the reality condition of the three zeroes for $\gamma\to 5/3$ and small ξ requires that $\xi=O(5-3\gamma)^2$, so that the three critical points in equation (C6) collapse into the origin for $\gamma\to 5/3$, consistently with the general result of Appendix B for adiabatic accretion.

C2 Dependence on the galaxy mass

A different situation is obtained when considering equation (C4) as a function of $\mathcal{R}$. It is apparent how $R>0$ for $\mathcal{R}\to 0$, and there is only one real solution, as expected, because the problem reduces to the classical Bondi problem. The perturbed position of the minimum can be determined again from Appendix A, with x_0 given in equation (27). Instead, $R<0$ for very large values of $\mathcal{R}$ and $\gamma>1$, and so equation (C2) admits three real solutions. Descartes' sign rule shows that the three zeros are positive. By using the order-balance technique it can be shown that their asymptotic leading term at fixed γ and ξ (in order of increasing distance from the centre) is given by

$$x_1\sim\frac{\chi\xi(5-3\gamma)}{4(\gamma-1)\mathcal{R}},\quad x_2\sim\frac{4\xi(\gamma-1)}{5-3\gamma},\quad x_3\sim\frac{(5-3\gamma)\mathcal{R}}{4}. \tag{C7}$$

One could be worried by the possibility that for $\gamma\to 5/3$, the solution x_2 becomes larger than x_3: however, it can be shown that once the reality condition is verified this cannot happens, because in order to have $R<0$, the mass ratio $\mathcal{R}$ must diverge faster than $(5-3\gamma)^{-2}$ for $\gamma\to 5/3$. The $\gamma=1$ case is discussed in the following section.

As an interesting application of the results of this Appendix, note how the radius $r_{\rm B,eff}$ defined in equation 6 of Park et al. (2016) is just the true sonic radius, except for a factor equal to $(5-3\gamma)/4$, in the two limits of very large bulge mass or very large core radius; this comes from using the results found here for the sonic radius, in the two limits.

C3 The isothermal case

A particularly simple case is the isothermal one. In fact, for $\gamma=1$ equation (C4) leads to the study of the sign of the quadratic polynomial $\chi\mathcal{R}^2+(2\chi^2-10\chi\xi-\xi^2)\mathcal{R}+(\chi+2\xi)^3$. Therefore, at variance with the $\gamma>1$ cases, in isothermal accretion $R>0$ for large values of $\mathcal{R}$ and fixed ξ, and only one (positive) minimum exists, with the sonic point given by the last identity in equation (C7) with $\gamma=1$. In addition, $R>0$ for large values of ξ and fixed $\mathcal{R}$, with the sonic point placed at $x_{\rm min}$ in equation (27) with $\gamma=1$. Finally $R>0$ independently of $\mathcal{R}$ when $\xi<4\chi$, and so again there is only one (positive) minimum. For $\xi\geq 4\chi$, there are two positive values of the galaxy-to-MBH mass ratio

$$\mathcal{R}_{\rm max,min}=\frac{-2\chi^2+10\chi\xi+\xi^2\pm\sqrt{\xi(\xi-4\chi)^3}}{2\chi}, \tag{C8}$$

so that $R<0$ for $\mathcal{R}_{\rm min}<\mathcal{R}<\mathcal{R}_{\rm max}$: Descartes' sign rule shows that the three zeros are all placed at $x>0$. In particular, for $\xi\to\infty$, $\mathcal{R}_{\rm min}\sim 8\xi$ and $\mathcal{R}_{\rm max}\sim\xi^2/\chi$. Summarizing, in the isothermal case, for $\xi<4\chi$ there is only one minimum $\forall\mathcal{R}>0$, for $\mathcal{R}<27\chi$ there is only one minimum $\forall\xi>0$, and there is only one minimum for large values of $\mathcal{R}$ (ξ) and fixed ξ ($\mathcal{R}$). The situation is clearly illustrated in Fig. C1.

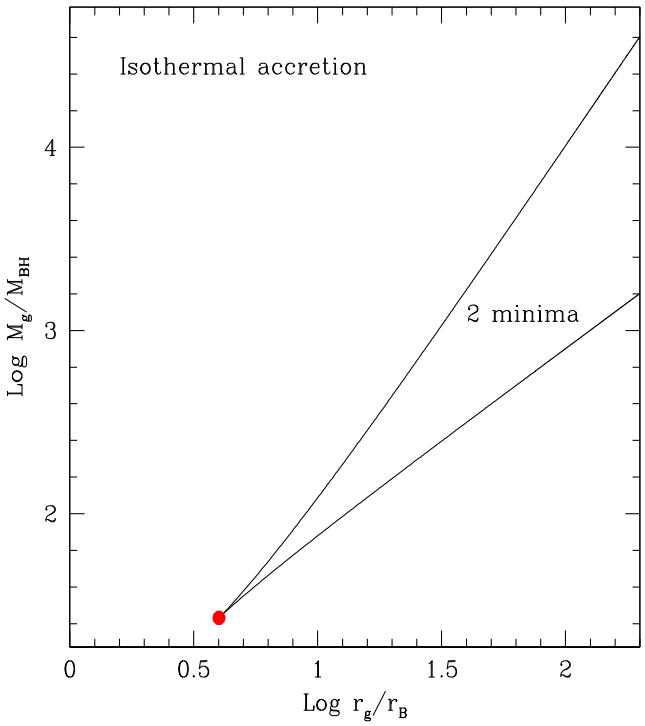

Figure C1. Parameter space for the existence of minima relative to the isothermal Bondi accretion in a Hernquist galaxy. For simplicity the effect of electron scattering is not taken into account, i.e. we assume $\chi = 1$ in equation (C2). The two solid lines show the boundaries given by equation (C7): in the region between the two lines the problem presents three positive zeroes, corresponding to two minima and one maximum. Outside the infinite triangular regions only one minimum exists. The coordinate of the red dot are $(\xi, \mathcal{R}) = (4, 27)$. Note that for the fiducial values (100, 1000) the accretion presents two minima.

This paper has been typeset from a TEX/LATEX file prepared by the author.